THE JOURNAL OF PHYSICAL CHEMISTRY B

Article

Cite This: J. Phys. Chem. B 2019, 123, 10233−10244

pubs.acs.org/JPCB

Exploring with Molecular Dynamics the Structural Fate of PLGA Oligomers in Various Solvents

James Andrews and Estela Blaisten-Barojas*

Center for Simulation and Modeling (formerly, Computational Materials Science Center) and Department of Computational and Data Sciences, George Mason University, Fairfax, Virginia 22030, United States

Supporting Information

ABSTRACT: This study focuses on the solvent effects that promote preferred solvated structures of polylactic-*co*-glycolic acid (PLGA) oligomers of molecular weight 278, 668, and 1449 u in ethyl acetate, water, and a mixture of both solvents. Our methodology consists of all-atom, explicit solvent molecular dynamics simulations for inspection of the solvated oligomer structures at ambient conditions. Parameters for the generalized Amber force field are developed in this work for the ethyl acetate liquid and the PLGA oligomers. Energetics, oligomer radius of gyration, end-to-end distance, orientational order parameter, flexibility coefficient, and backbone dihedral angles are reported along with a size scaling property yielding a power law for PLGA oligomers in each of the three solvents considered. It is found that the PLGA oligomer has two characteristic states identified by a set of extended structures and a set of collapsed structures, the former being energetically preferred in ethyl acetate and its mixture with water. The two types of PLGA structures occur in the three solvents and although they flip from one to the other in a sporadic fashion, in ethyl acetate, the extended structures may persist for more than 20 ns. The collapsed structures are significantly more frequent in water, occurring seldom in the mixed ethyl acetate−water solvent. PLGA is a biodegradable polymer approved for use in pharmaceutical and biomedical applications. Insights provided therein are of importance for the polymer aggregation process and its glassy state in condensed phases.

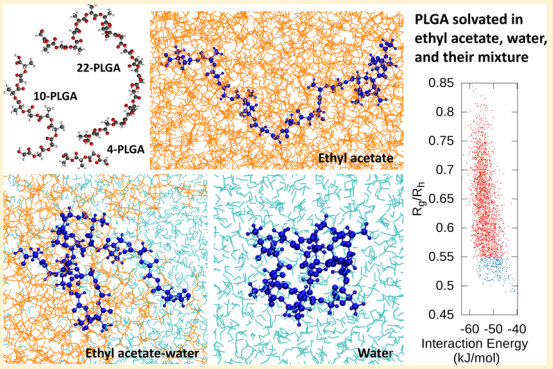

1. INTRODUCTION

Interest in biodegradable polymers for medicinal applications and in polymers from renewable resources is a major focus in the search for novel well-defined macromolecular nanoparticles. Polymeric nanoparticles formed from polylactic-*co*-glycolic acid (PLGA) constitute a vast class of soft matter nanostructures of exceptional technological significance for drug delivery and tissue engineering applications.[1] PLGA is soluble in ethyl acetate (EA), the organic solvent commonly used for the fabrication of nanoparticles.[2,3] On the other hand, PLGA undergoes hydrolysis in water by degrading into oligomers of various sizes.[2,4] Oligomers of PLGA are also synthesized at specific molecular weights in applications such as the manufacture of tablets and pellets where drugs are added to molten oligomeric PLGA and solidified later.[5] However, the molecular solvation and thermodynamic character of specific polymer oligomers in these macrostructures remain basically unknown.

There are only a few molecular-scale studies of monodisperse dimers, tetramers, and larger oligomers of lactides and glycolides,[6,7] but none for their PLGA copolymer. Although the solvated behavior of oligomers is important for understanding the formation mechanism of PLGA nano and microparticles, the field has remained mostly empirical.[8,9] Molecular-scale simulation techniques are promising methodologies as a way forward for designing nanoscale drug delivery systems.[10,11] Among them, molecular dynamics (MD) approaches are powerful tools for predicting and inspecting structural, thermal, and physical properties such as the polymer glass transition temperature T_g of polymers at the molecular scale.[10] Therefore, a detailed study of short PLGA oligomers from an all-atom perspective in relevant solvent media is currently due.

In fact, analysis of PLGA oligomeric nanostructures stabilized by solvents entails an unprecedented opportunity for impacting materials design and simultaneously contributes to the fundamental understanding of the solvent effects on the structure of solvated polymer chains. The focus of this paper is on analyzing the effect that three solvents, EA, water, and their mixture, have on the energetics, structure, and thermodynamic properties of 50:50 PLGA oligomers via all-atom MD simulations in an explicit solvent. We analyze three PLGA sizes with molecular weights of 278, 668, and 1449 u. We find that two prototypical oligomer structures occur during the simulation time. One structure is elongated with kinks and twists, and the other has a bent, collapsed shape. The collapsed structures occur more frequently when the oligomers are in

Received: July 14, 2019
Revised: November 5, 2019
Published: November 8, 2019

DOI: 10.1021/acs.jpcb.9b06681
J. Phys. Chem. B 2019, 123, 10233−10244

Table 1. $PLGA_{50:50}$ Sequence of Lactic/Glycolic Acids of the Oligomers Studied in This Work Showing the Random Distribution of Their Monomer Types[a]

oligomer	model	sequence	ratio L-:D-	mass (u)	no. of atoms
22-PLGA	A	LGLGGDLGGDGGLGLDLGLGLG	8:3	1449.1	168
22-PLGA	B	LGLGLDLDGGLDGGGGGDGDLG	6:5	1449.1	168
22-PLGA	C	LGGGGDGGLGLDLDLGLDGGLG	7:4	1449.1	168
10-PLGA	I	LGLDGDLGGG	3:2	668.5	78
10-PLGA	J	LGGDGDLGLG	3:2	668.5	78
10-PLGA	K	LGGDLDGDGG	2:3	668.5	78
4-PLGA		LDGG	1:1	278.2	33

[a]The L- and D-lactic acid enantiomers are referred as L and D, respectively. The glycolic acid monomers are referred as G.

Table 2. Structural Properties of the Extended Initial PLGA Oligomers

Oligomer	R_g (nm)	R_{hyd} (nm)	R_{ee} (nm)	Z	C_R	I_A (u·nm^2)	I_B/I_A	I_C/I_A
22-PLGA model A	2.3	2.3	7.8	0.95	45	25.3	300.0	300.3
22-PLGA model B	2.3	2.3	7.8	0.95	45	31.1	245.1	245.8
22-PLGA model C	2.2	2.3	7.8	0.94	45	28.9	255.1	255.2
10-PLGA model I	1.0	1.3	3.6	0.95	21	8.8	81.8	82.4
10-PLGA model J	1.1	1.4	3.6	0.95	21	8.9	83.4	84.0
10-PLGA model K	1.0	1.3	3.6	0.94	21	9.2	78.3	80.0
4-PLGA	0.5	0.8	1.4	0.93	8	3.5	15.0	15.5

water, and the extended structure forms more frequently when the oligomers are in EA, showing that a preferential compact shape is favored in the polar solvent. However, oligomers in the EA−water mixed solvent get trapped with mostly extended structures at the interface of the liquid−liquid phase-separated EA−water mixed solvent. This classification is of particular interest for the determination of PLGA oligomers produced when the polymer is dissolving in EA or when hydrolyzing in water. Additionally, the local structure of oligomers impacts T_g and the structure of asymmetric nanoparticles.[9]

This manuscript is organized as follows. Section 2 provides a description of the MD parameters and force field used. Sections 3−5 present the energetics, structure, and properties found for the PLGA oligomers solvated in EA, water, and the mixture of both solvents, respectively. These sections present analyses of the PLGA structure with respect to system size across tens of nanoseconds of dynamic evolution. Section 6 provides a discussion comparing the effects of the solvent local environment around the PLGA oligomers. Section 7 concludes this work. The Supporting Information contains the generalized Amber force field (GAFF) new parameters and provides a collection of plots with the time dependency of the PLGA calculated properties.

2. METHODS

Here, we have considered three molecular weights of $PLGA_{50:50}$ as the solute in three molecular solvents, EA, water, and their mixture. $PLGA_{50:50}$ is widely used and is well-studied experimentally.[12,13] In $PLGA_{50:50}$, the number of lactic acid monomers is equal to the number of glycolic acid monomers. Lactic acid has two stereoisomers, L- and D-, that differ on the asymmetric α-carbon. The polymer matrix of $PLGA_{50:50}$ is amorphous[14] and displays a random distribution of L- and D-lactic acid enantiomers,[13] with physicochemical properties approximately identical independently of the enantiomer relative concentration.[15] The smallest oligomer considered is 4-PLGA with four monomers, has chemical formula $C_{10}H_{14}O_9$, and molecular weight 278.2 u. The two larger oligomers considered are 10-PLGA including 10 monomers ($C_{25}H_{32}O_{21}$) with molecular weight 668.5 u and 22-PLGA having 22 monomers ($C_{55}H_{68}O_{45}$) with molecular weight 1449.101 u. For these larger oligomers, three different lactic/glycolic isomers of randomized sequences are considered as described in Table 1.

Force field parameters for the EA molecules and the PLGA oligomers are developed using the AmberTools16[16] utilities and the all-atom GAFF with the Morse potential for the bond terms. Two sets of charges are calculated, the AM1-BCC additive bond charge corrections[17,18] intrinsic to the AMBER16 tools and the restrained electrostatic potential (RESP) charge scheme based on the Merz−Singh−Kollman population[19,20] calculated separately at the B3LYP 6-31G* density functional theory via Gaussian 09.[21] PLGA oligomers are zwitterions sustaining a localized charge of about −0.19 e on the L end-monomer and +0.19 e on the G end-monomer. The TIP3P[22] and SPC/E[23] models are used for water simulations. MD simulations are performed with the GROMACS 2018.2 package[24] in double precision. Topology files with the GAFF parameters with RESP charges are provided in the Supporting Information.

While there are extensive simulations on water as a solvent, this is not the case for EA. Thus, a preliminary MD study of this liquid is undertaken for the pure EA system as described in Section 3 for several of its properties. Each solute/solvent system has a 1.36% concentration by mass of PLGA in the respective solvent. In water, the 4-, 10-, and 22-PLGA oligomers are solvated with the same 1.36% concentration by mass. The third case is a mixed EA−water solvent with relative concentration by mass of 38:62 (1:1.63), such that the PLGA overall concentration by mass is 0.96% for 10- and 22-PLGA and 1.02% for 4-PLGA.

Two simulation stages are performed for each system. The first stage involves conducting *NPT* MD of the solute in explicit solvents for equilibrating the system to the desired thermodynamic state with the Berendsen thermostat and barostat. A time step of 1 fs, periodic boundary conditions (PBC), and cutoff radii of 1.4 nm are used throughout along 20 ns of equilibration, which ensured fluctuations in the density of 3−5 kg/m^3. Ewald sums are used in all calculations for the long-range electrostatics within the particle mesh implementation (PME). The second

DOI: 10.1021/acs.jpcb.9b06681
J. Phys. Chem. B 2019, 123, 10233−10244

stage consists of production *NVE* runs for each system of 40 ns at its equilibrated density and temperature. During production, configurations of the full system are saved for postanalysis intended to capture the slow changes of several structural characteristics of the solvated PLGA oligomers. Postanalysis of the system energetics consists of calculating the total potential energy of all molecules in the box for each saved configuration, PE_{total}, the potential energy of the PLGA oligomer without the solvent, PE_{PLGA}, and the potential energy of the solvent without the PLGA oligomer, $PE_{solvent}$, such that an interaction energy E_{int} between the solvent and solute is defined as $E_{int} = PE_{total} - (PE_{solvent} + PE_{PLGA})$.

Several structural properties of the polymer are examined such as the mass-weighted radius of gyration $R_g^2 = \sum_{i=1}^{N}(\mathbf{r}_i - \mathbf{r}_{cm})^2/N$ and the hydrodynamic radius $R_{hyd}^{-1} = \frac{1}{N^2}\sum_{i=1}^{N-1}\sum_{j>i}^{N} r_{ij}^{-1}$, where $\mathbf{r}_i$ is the position of atom i referred to the polymer center of mass, r_{ij} is the distance between atoms i and j, and N is the number of atoms in the oligomer. The orientation order parameter describes how random are the orientation angles α_i of vectors connecting contiguous monomers with respect to the oligomer director vector joining the polymer ends,[25,26] $Z = \frac{3}{2(n-1)}\sum_{i=1}^{n-1}\cos^2\alpha_i - \frac{1}{2}$, where n is the number of oligomer monomers. A fully stretched out oligomer has $Z = 1$, while $Z = 0$ indicates random orientations with respect to the director vector. A useful property for a polymer with N_{bb} bonds in its backbone is the characteristic ratio C_R between the mean squared end-to-end distance $\langle R_{ee}^2\rangle = \left\langle \sum_{i=1}^{N_{bb}}\sum_{j=1}^{N_{bb}} l_i \cdot l_j \right\rangle$ and the mean squared backbone bond length $\langle l^2\rangle$, $C_R = \langle R_{ee}^2\rangle/(N_{bb}\langle l^2\rangle)$.[27]

Other structural properties are the oligomer moments of inertia along the molecular principal axes, which provide some information of the molecular shape as the spherical top when the three moments are equal, oblate symmetric top if $I_A > I_B = I_C$, or prolate symmetric top for $I_A < I_B = I_C$. Diffusion coefficients D of the oligomers in various solvents and D_s the self-diffusion coefficient of EA are derived from the Einstein relation and corrected by D_{PBC} due to the periodic boundary conditions imposed to the system

$$D = \frac{1}{6t}\frac{1}{m}\sum_{\alpha=1}^{m}\frac{1}{n}\sum_{i=1}^{n}(\mathbf{r}_i(t) - \mathbf{r}_i(t_\alpha))^2 + D_{PBC} \quad (1)$$

where $\mathbf{r}_i(t)$ is the position of the ith monomer center of mass at time t. Each *NVE* run is split into m time series, each series starting from a reference position $\mathbf{r}_i(t_\alpha)$ and their average is taken as indicated in eq 1. The last term in eq 1 accounts for a correction due to the periodic boundaries,[28] $D_{PBC} = \frac{k_B T\xi}{6\pi\eta L}$, where k_B is Boltzmann's constant, T is temperature, $\xi = 2.837297$, L is the computational box length, and η is the solvent viscosity. The latter are taken from the experimental values $\eta_{water} = 0.8937$ mPa·s and $\eta_{EA} = 0.441$ mPa·s.[29]

As a reference for simulations described in the upcoming sections, the initial values of the structural properties of the extended PLGA oligomers are given in Table 2. Initially, the oligomers are prolate symmetric tops.

3. PURE ETHYL ACETATE

Before solvating the PLGA oligomers in EA, we validate the force field parameters for the liquid and compare simulation results of the pure liquid EA with available experiments. The agreement is very good, with a correlation coefficient of 0.85. A pure EA system of 232 molecules was equilibrated at 298 K and 1.013 bar with *NPT* MD considering the two sets of charges for the EA molecule, BCC and RESP. These simulations yielded equilibrium densities of 923 ± 5 kg/m^3 (BCC) and 907 ± 4 kg/m^3 (RESP) showing that the former is slightly above the experimental value of 902 kg/m^3.[29] A further *NVT* production run at that density and temperature yields a heat capacity at a constant volume of 175 J/mol/K, in agreement with experiments of 170 J/mol/K.[30] In addition, from *NVE* runs of 5 ns and 25 time origins, the self-diffusion coefficient D_s of eq 1 yields values of $(1.78 \pm 0.01) \times 10^{-5}$ cm^2/s (BCC) and $(1.96 \pm 0.07) \times 10^{-5}$ cm^2/s (RESP), including a PBC correction of 0.44×10^{-5} cm^2/s. The estimated value of D_s is in between the only experimental value found in the literature of $(2.77 \pm 0.09) \times 10^{-5}$ cm^2/s[31] and the estimate of 1.19×10^{-5} cm^2/s derived from the Wilke−Chang empirical correlation[32] for the Stokes radius.[33] Furthermore, a more fundamental validation of the force field parameters is conducted from the *NVE* simulation by selecting randomly 65 molecules and their GAFF potential energy compared with binding energies calculated with density functional theory at the B3YLP/6-311++G(d,p) level.[21] The agreement is very good, with a correlation coefficient of 0.85.

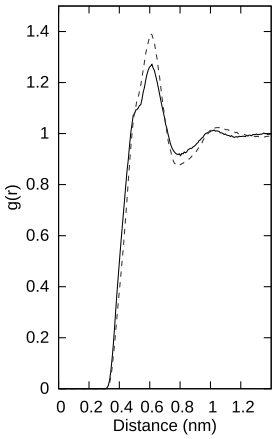

Figure 1. rdf of EA, at 298 K 923 kg/m^3 (BCC, dashed line) and 907 kg/m^3 (RESP, solid line). The plot depicts distances between centers of mass of the EA molecules.

The MD average potential energy per EA molecule is −100.37 kJ/mol (BCC) and −324.54 kJ/mol (RESP). On average, the radius of gyration of the EA molecules is 0.235 nm, $R_{ee} = 0.461$ nm, $Z = 0.77$, and the molecular director vectors are distributed randomly yielding a zero S order parameter as is characteristic in a molecular liquid.[34] The EA molecules are prolate almost symmetric tops with moments of inertia along the principal axes of 64 ± 6, 236 ± 17, and 277 ± 25 u Å^2. Figure 1 illustrates the radial distribution function (rdf) of the EA molecule centers of mass showing that the first coordination shell in this liquid is broad with distances between molecules ranging from 0.4 to 0.65 nm.

To the best of our knowledge, there is only one other simulation of pure EA[35] in which the GAFF force field was used but with parameters different than the ones we have defined. As a comparison, we run simulations with the Caleman et al.[35] parameters under the same conditions as ours and obtained an equilibrium density of 933 ± 9 kg/m^3 and a constant volume heat capacity of 164.5(0.2) J/mol/K, which are comparable to our BCC results. However, their equilibrium density is significantly higher than both the experimental value[29] and

DOI: 10.1021/acs.jpcb.9b06681
J. Phys. Chem. B 2019, 123, 10233−10244

our RESP results of 907 ± 4 kg/m^3. Additionally, the reported self-diffusion coefficient of (1.510 ± 0.001) × 10^{-5} cm^2/s is more discrepant from the experimental measurement[31] and 15% (BCC) or 23% (RESP) lower than the values obtained from our GAFF parameters.

4. PLGA OLIGOMERS IN ETHYL ACETATE

The MD *NPT* simulations at 298 K and 1.013 bar of the various PLGA oligomers solvated in EA yield an equilibrium density of

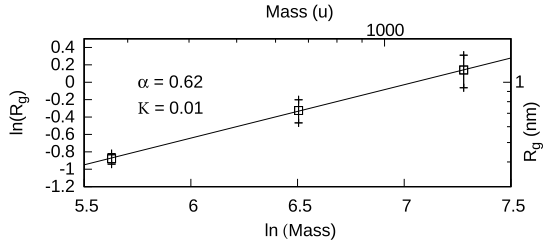

Figure 2. Relationship between radius of gyration and molar mass of the polymer as described by eq 2 for PLGA oligomers in EA. The exponent is $\alpha = 0.62$ and the proportionality coefficient is $K = 0.01$ nm/u$^{0.62}$. The error is 0.008.

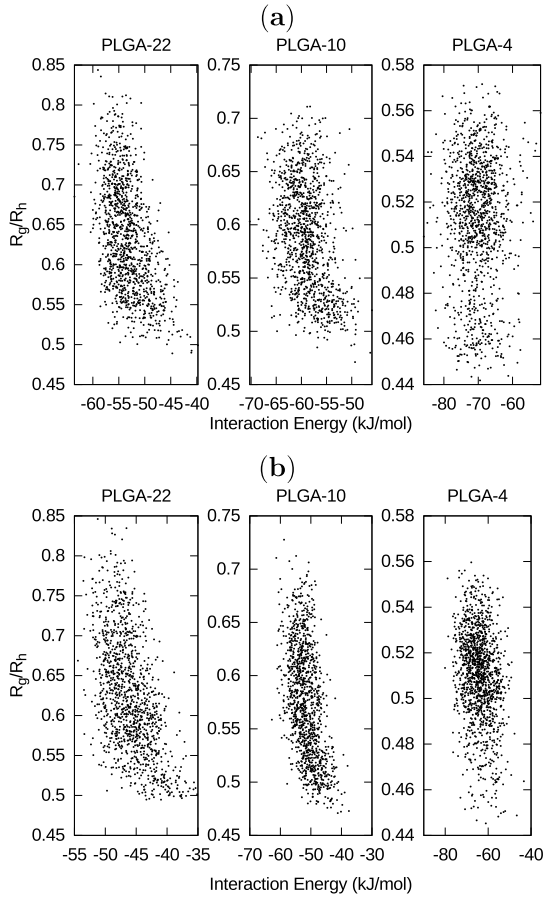

Figure 3. Ratio of the radius of gyration to the hydrodynamic radius of the PLGA oligomers in EA solution vs interaction energy per monomer along the 40 ns MD *NVE* runs of the seven different oligomers combined in one plot per size at 298 K. (a) BCC charges and (b) RESP charges.

921 ± 3 kg/m^3 (BCC) and 912 ± 3 kg/m^3 (RESP), which are acquired in computational boxes containing 1204, 557, and 232 EA molecules and one 22-, 10-, or 4-PLGA oligomer. Once equilibrated, each of the systems is followed with MD-*NVE* for at least 40 ns and configurations are recorded every 100 fs for further analyses. Along this time evolution, the temperature fluctuates slightly between 298 ± 2 K and the PLGA oligomers lose their initial fully elongated conformation and become more compact. For example, the R_g shrinks by more than half. The initial prolate symmetric top shape given by the moments of inertia persists, but the ratios I_B/I_A, I_C/I_A decrease by two and one orders of magnitude for the 22-PLGA and 10-PLGA, respectively, and by a factor of 4 for 4-PLGA. The oligomer end-to-end distance R_{ee} is smaller than its full polymer length and displays very large fluctuations as an indication that the polymers are flexible while in solution. In fact, the flexibility coefficient C_R decreases to values of about 6. The Z order parameter is very small, indicating a fairly random sequence of orientations between vectors joining contiguous monomers with respect to the end-to-end orientation vector. Averages of these properties coincide within the error for the BCC and RESP cases, as seen in the Appendix Table A1. Concerning the energetics, the oligomer potential energies are higher than the initial values while the solute−solvent interaction energies E_{int} are negative indicating a stabilizing environment for oligomers immersed in the EA solvent. Both BCC and RESP cases result in similar E_{int}, with the latter being about 7 kJ/mol lower. Averages of the energetics are given in the Appendix, Table A1.

Solvated linear polymers display a power law between radius of gyration and mass with a particular scaling exponent α for each solvent[27]

$$R_g = KM_W{}^{\alpha} \tag{2}$$

where M_W is the mass of the polymer and K and α are constants. For solvated polymers in a good solvent, the scaling exponent α is expected to be 3/5, while polymers in poor solvents are expected to have α = 1/3.[36] Chains in a good solvent favor interactions with the solvent over intramolecular interactions and extend, while polymers collapse in a poor solvent and fill densely the volume they occupy. Theoretically, the scaling exponent α is known for several common molecular shapes, including 1/3 for a sphere, 1/2 for a random coil, and 1 for an extended rod.[37] This scaling behavior is satisfied for the PLGA oligomers, for both BCC and RESP cases, and Figure 2 shows that EA is indeed a good solvent with α = 0.62 and proportionality factor K = 0.01 nm/u$^{0.62}$.

Calculated diffusion coefficients D of the PLGA oligomers in EA are 0.51 ± 0.01, 0.61 ± 0.01, and 0.80 ± 0.02 × 10^{-5} cm^2/s (BCC) and 0.60 ± 0.01, 0.76 ± 0.01, and 0.94 ± 0.01 × 10^{-5} cm^2/s (RESP) for 22-, 10-, and 4-PLGA, respectively. These diffusion coefficients are obtained from averages of the oligomer MSD across 200 ps strides split from the full *NVE* simulation times for each oligomer size and include the correction for PBC. As expected, the oligomer diffusion coefficients decrease as the larger is the oligomer, and our predicted values are on the order of the diffusion coefficients of similar polymers.[38] Although the PLGA oligomers are not spherical, the Stokes radius of an equivalent sphere diffusing in the solvent can be calculated from $R_{Stokes} = k_BT/(6\pi\eta_{EA}D)$ using the D from the simulation and the EA experimental viscosity. The resulting R_{Stokes} are 1.07, 0.90, and 0.68 nm (BCC) and 0.92, 0.73, and 0.60 nm (RESP) for the three oligomer sizes in decreasing order. The overall signature of the diffusing polymers in the EA molecular liquid is that of "effectively smaller objects" diffusing in a faster moving solvent for the RESP model when compared to the BCC model.

DOI: 10.1021/acs.jpcb.9b06681
J. Phys. Chem. B 2019, 123, 10233−10244

Table 3. Property Averages of the PLGA Oligomers Extended and Collapsed Structures When Solvated in EA[a]

	extended			collapsed		
property	22-PLGA	10-PLGA	4-PLGA	22-PLGA	10-PLGA	4-PLGA
R_g (nm)	1.2 ± 0.2	0.77 ± 0.07	0.43 ± 0.01	0.83 ± 0.06	0.60 ± 0.04	0.39 ± 0.02
R_{hyd} (nm)	1.8 ± 0.1	1.25 ± 0.04	0.80 ± 0.01	1.57 ± 0.08	1.14 ± 0.05	0.78 ± 0.02
R_{ee} (nm)	2.9 ± 1.0	2.1 ± 0.5	1.1 ± 0.1	1.6 ± 0.5	1.0 ± 0.4	0.9 ± 0.2
Z	0.1 ± 0.1	0.2 ± 0.2	0.6 ± 0.1	0.0 ± 0.1	0.0 ± 0.1	0.3 ± 0.2
I_A/I_A	1.0 ± 0.3	1.0 ± 0.3	1.0 ± 0.2	1.0 ± 0.2	1.0 ± 0.2	1.0 ± 0.2
I_B/I_A	4.1 ± 1.7	4.7 ± 1.2	5.7 ± 0.6	1.7 ± 0.3	2.0 ± 0.3	3.0 ± 0.5
I_C/I_A	4.7 ± 1.6	4.3 ± 1.0	6.1 ± 0.5	2.2 ± 0.3	2.6 ± 0.4	3.5 ± 0.4
PE_{BCC} (kJ/mol)	62 ± 3	63 ± 3	71 ± 5	59 ± 3	61 ± 4	70 ± 5
PE_{RESP} (kJ/mol)	67 ± 6	79 ± 4	124 ± 5	63 ± 6	75 ± 5	123 ± 5
$E_{int_{BCC}}$ (kJ/mol)	−54 ± 3	−60 ± 3	−71 ± 5	−50 ± 4	−57 ± 4	−69 ± 5
$E_{int_{RESP}}$ (kJ/mol)	−47 ± 3	−54 ± 3	−69 ± 5	−42 ± 3	−49 ± 4	−68 ± 6

[a]Averages of structural properties are the same for the BCC and RESP charges. Energies are per monomer.

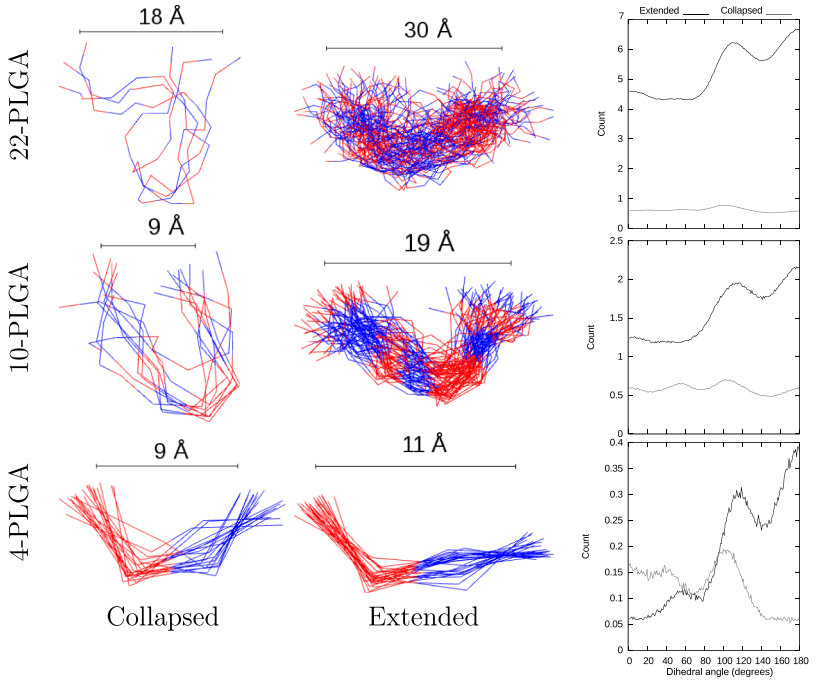

Figure 4. Left panes: Wireframe view of monomer centers of mass of PLGA oligomers in EA partitioned by *collapsed* and *extended* structures. The number of displayed chains is proportional to their frequency in the simulation. Lactic acid monomers are depicted red and glycolic acid monomers are blue. Right pane: distribution of the dihedral angles in the partitioned structures; black lines correspond to the extended structures and gray lines to the collapsed structures. The distribution of dihedral angles in TIP3P (shown) and SPC/E waters is basically the same.

It is known that the ratio between averages $\langle R_g^2\rangle/\langle R_{ee}^2\rangle = 1/6$ is achieved when the polymer is randomly coiled.[36] However, the PLGA oligomers in EA acquire ratios spanning between 0.06 and 0.45, clearly indicating that these polymer chains are not randomly coiled most of the time. Another popular ratio is $R_g/R_{hyd} = (3/5)^{1/2} \approx 0.77$, which corresponds to a solid sphere[39,40] and is used for identifying globular proteins in solution. The spherical shape is not the case for the PLGA oligomers either because the three oligomer sizes display ratios mostly below 0.77 for their accessible states along the simulation time, as shown in Figure 3. To be noted from this figure is that the small R_g/R_{hyd} ratios have a higher polymer−solvent interaction energy than the large ratios, which suggests that the solvent stabilizes better those structures leading to high ratios. Considering R_{hyd} calculated from distances between the polymer monomer centers of mass instead than from atomic distances gives a coarse grained overall view of the oligomers. Using the coarse grained values, and taking into account the different oligomer sizes, the related ratio $R_{Stokes}/R_{hyd} \approx 0.54-0.50$ led us to define two characteristic structures of the oligomers in the EA solution: extended structures when $R_g/R_{hyd} \gtrsim 0.54$ and *collapsed* structures when $R_g/R_{hyd} \lesssim 0.54$. PLGA oligomers in EA most frequently acquire the *extended* structures, with 89, 73, and 60% appearances for the 22-, 10-, and 4-PLGA oligomers, respectively. The shorter the oligomer, the more frequently the structure undergoes a change. The extended structures of 22-PLGA may remain unchanged for as long as 20 ns while the collapsed structure is kept for at most 1 ns. Table 3 gives the structural properties of the PLGA oligomers once the structures along the simulation are split into extended and collapsed, showing clearly the important differences between them. The moments of inertia present high fluctuations, indicating that there is a diversity of possible rotations that the structure may have either when extended or collapsed. On the other hand, the

DOI: 10.1021/acs.jpcb.9b06681
J. Phys. Chem. B 2019, 123, 10233−10244

energetic properties are very similar between the two sets of structures. The Supporting Information contains plots of the time dependence of the PLGA properties.

Figure 4 illustrates schematically the extended and collapsed structures. To visualize the change in the oligomer shape, other quantities are relevant such as the distribution of dihedral angles between every four contiguous monomer centers of mass of each oligomer, as shown in Figure 4 (right). This distribution shows clear peaks at 120 and 180° across the three oligomer sizes, which are attributed to extended chains (180°) and angular turns (120° and lower angles) needed when the oligomer chain bends into the collapsed structure. Interestingly and consistently with Figure 4, 4-PLGA is the most extended prolate top.

5. PLGA OLIGOMERS IN WATER

The PLGA oligomers solvated in TIP3P and in SPC/E water were *NPT* equilibrated at constant temperature and pressure of 298 K and 1.013 bar and reached equilibrium densities of 990 ± 2 kg/m^3 and 1002 ± 2 kg/m^3, respectively. These simulations had computational boxes with 5908, 2729, and 1134 water molecules and one 22-, 10-, and 4-PLGA oligomer, respectively. The equilibrium density in TIP3P water is lower because pure TIP3P water has a lower equilibrium density of 984 kg/m^3 than the 997 kg/m^3 of SPC/E water.[41,42] Next, the system was simulated with *NVE* MD at the equilibrium density, which maintained a temperature of 298 ± 1 K during production runs of 40 ns for each one of the seven PLGA oligomers in water. Configurations of the full system were recorded every 100 fs. Across all structural properties, PLGA oligomers in both waters have lower standard deviations than in EA, suggesting less structural variety along the trajectories. Noticeably, the flexibility coefficient C_R is about half of that in EA, pointing out to an enhanced chain flexibility as compared with the oligomer behavior in EA. Indeed, averages of both R_g and R_{hyd} are very similar to the values of the collapsed structures in EA, suggesting that most of the time the polymer structure in water is collapsed. While the oligomer potential energies are basically the same as when solvated in EA, the interaction energy with the solvent of the smaller oligomers has decreased, suggesting an enhanced stabilization of collapsed structures by the surrounding water molecules. Actual comparison of the structural and energetic properties between the two water models and the two sets of charges is provided in the Appendix table.

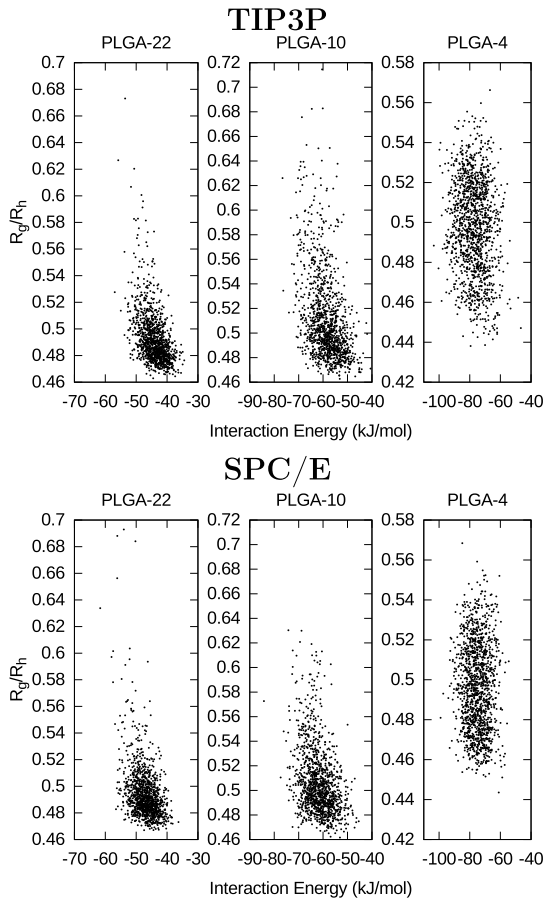

Figure 5. Ratio of the radius of gyration to the hydrodynamic radius of the PLGA oligomers in water solution vs interaction energy per monomer along the 40 ns MD *NVE* runs at 298 K of the seven different oligomers with RESP charges combined in one plot per size. Top: TIP3P, bottom: SPC/E.

The calculated diffusion coefficients D of the PLGA oligomers in TIP3P water are 0.88 ± 0.01, 1.13 ± 0.01, and 1.29 ± 0.01 × 10^{-5} cm^2/s (BCC) and 0.88 ± 0.01, 1.14 ± 0.02, and 1.45 ± 0.41 × 10^{-5} cm^2/s (RESP), for the 22-, 10-, and 4-PLGA, respectively. As expected, because SPC/E water has a self diffusion coefficient of 2.8 × 10^{-5} cm^2/s that is about 50% lower than the corresponding one of TIP3P water,[42] the D of the solvated oligomers are also lower than that in TIP3P water with values 0.49 ± 0.01, 0.64 ± 0.01, and 0.86 ± 0.02 × 10^{-5} cm^2/s for the three oligomers with decreasing size and RESP charges. These values include the PBC correction and are obtained as MSD averages considering 200 time origins across 40 ns runs for each of the seven oligomers. Our results are consistent with experimental diffusion coefficients of similar polymers such as lactic acid in aqueous solutions.[43] Additionally, the 4-PLGA diffusion coefficient compares well with simulations of similar size oligomers in TIP3P water such as 4-monomer oligomers of pure lactic acid (1.006 ± 0.032) × 10^{-5} cm^2/s and of pure glycolic acid (1.194 ± 0.062) × 10^{-5} cm^2/s.[38]

The power law of eq 2 giving the scaling between radius of gyration and mass is also satisfied for the PLGA oligomers in either water, TIP3P, or SPC/E, yielding an exponent α = 0.40, a proportionality coefficient K = 0.01 nm/u$^{0.41}$, and error of around 0.05. The exponent α is lower than that in the EA case, indicating that the oligomer mass is filling almost in full the volume it occupies. Therefore, water is a poor solvent for PLGA.

The range of oligomer states accessible in water and yielding R_g/R_{hyd} ratios is depicted in Figure 5, which shows more states with low than with high ratio. For example, the longer oligomer, 22-PLGA, lacks entirely the most extended structures. Using the separating criterion between extended and collapsed oligomer structures based on the ansatz R_g/R_{hyd} > or < 0.54−0.50 permits calculation of properties for the two sets of structures. Indeed, in the two water models, the collapsed structures are dramatically favored for the three oligomer sizes with percentages at or about 91, 75, and 70% for the 22-, 10-, and 4-PLGA oligomers, respectively. The collapsed structures persist for periods as long as 7 ns, while the extended structures remain stable over less than 1 ns. To be noted is that 22-PLGA model B has a particularly different behavior, with collapsed structures remaining only about 4 ns and changing frequently to the extended structures. For the two water models, the overall property averages of the two sets of structures are almost identical to those reported for the EA case in Table 3, with the exception of the polymer−solvent interaction energies that yield

DOI: 10.1021/acs.jpcb.9b06681
J. Phys. Chem. B 2019, 123, 10233−10244

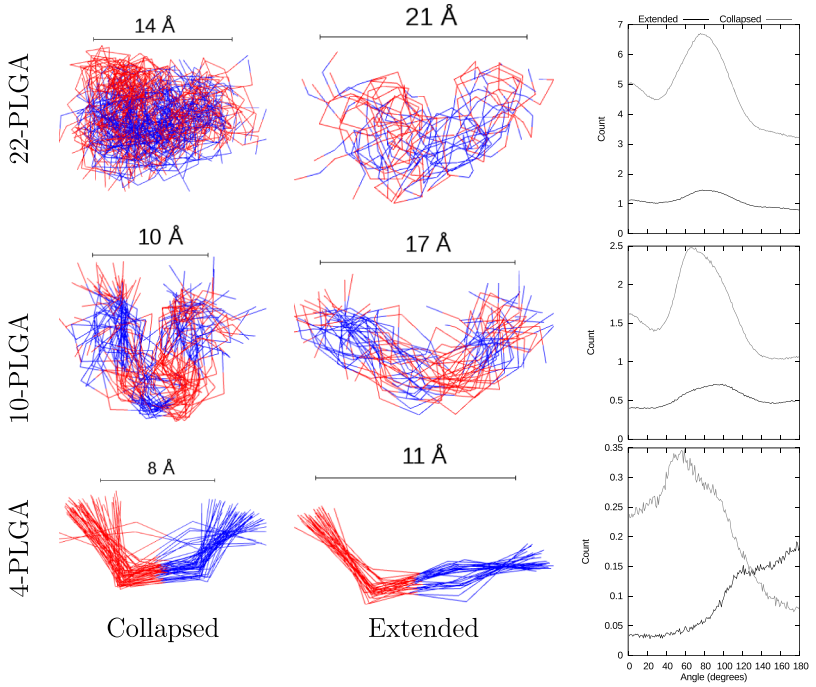

Figure 6. Left pane: Wireframe view of monomer centers of mass of PLGA oligomers in water partitioned by *collapsed* and *extended* structures. The number of displayed chains is proportional to their frequency in the simulation. Lactic acid monomers are depicted red, and glycolic acid monomers are blue. Right pane: distribution of the dihedral angles in the partitioned oligomer structures; black lines correspond to the extended structures, and gray lines to the collapsed structures. TIP3P (shown) and SPC/E waters yield very similar distributions for oligomers with either BCC or RESP charges.

up to about 10 kJ/mol additional solvent stabilization of the molecular structure in 10- and 4-PLGA. The Appendix Table A1 includes these averaged properties. Plots of the time dependency of the calculated PLGA properties for the various polymer models and sizes solvated in the two waters (TIP3P and SPC/E) are included in the Supporting Information. Figure 6 provides visualization of the extended and collapsed structures in water. To the left in this figure, the distribution of dihedral angles acquired along the simulation is depicted showing the dramatic predominance of angles below 120° in contrast with the distributions in the EA case of Figure 4. The distribution of oligomers dihedral angles is basically identical for the two water models.

6. PLGA OLIGOMERS IN MIXED EA–WATER SOLVENT

The third system studied is a 1:1.643 solvent mixture of EA–water. This solvent mixture has been used experimentally for the production of asymmetric PLGA nanoparticles.[9] The initial computational box is generated by randomly placing either EA or water molecules in a cubic lattice with the PLGA chain placed at the center. The systems are equilibrated with *NPT* MD during 20 ns at 298.15 K and 1.01325 bar, yielding an equilibrium density of 961 ± 3 kg/m^3 with TIP3P water and 1002 ± 3 kg/m^3 with SPC/E water. These systems were composed of 603/5454, 279/2519, and 116/932 EA/water molecules with one 22-, 10-, and 4-PLGA solute, respectively. At equilibrium, the two liquids phase-separate as expected because EA is only 0.064 kg/L soluble in water at 298.15 K.[44]

In general, the PLGA properties are in-between those of the oligomers solvated in EA and in either one of the two water models. However, the solvated oligomers in these mixed solvents have interaction energies with the solvent similar to those solvated in the corresponding water. Averaged values of the structural properties are provided in the Appendix table for BCC or RESP charge cases and for TIP3P water and SPC/E water. While PLGA oligomers prefer extended structures in EA and collapsed structures in water, PLGA oligomers in the mixed solvent alternates between both structures more evenly. The range of accessed structures are depicted in Figure 7 through the ratio between the gyration and hydrodynamic radii.

The separation between extended and collapsed structures based on the proposed ansatz yields 56, 59, and 58% of extended structures with BCC charges in EA-TIP3P water and 67, 64, and 63% with RESP charges for the 22-, 10-, and 4-PLGA, respectively. Meanwhile, in EA-SPC/E, the percentages of extended structures with RESP charges are 71, 63, and 65%. As expected, the average properties of the two sets of structures are similar to those reported in Table 3. Figure 8 illustrates instantaneous structures of the extended and collapsed PLGA structures. Overall, the longest intervals that 22-PLGA remains in each structure are about 7 ns for the extended structure and about 2 ns for the collapsed structure. Model B of 22-PLGA has a significantly different pattern of how the structure changes on time, displaying periods of 3 ns elongated but alternated with 2.5 ns lapses of collapsed structures. Interestingly, during the simulation, the PLGA oligomers remain most of the time confined to diffusing locally across the interface between the phase-separated solvents. Thus, because the PLGA oligomers are physically in two different local environments, the main overall mobility of the solute is similar to that of EA molecules. The Supporting Information contains plots of the time evolution of the oligomers in the mixed solvent EA-TIP3P and EA-SPC/E. Unforeseeably, the oligomers in the mixed solvent also display scaling with a power law as in eq 2 with exponent $\alpha = 0.51$ and proportionality factor $K = 0.02$ nm/u$^{0.51}$, although the 0.06 error of the fit is larger than that in the two previous cases. This exponent is very close to the theta-solvent of 0.5. However, these PLGA structures are not consistent with randomly coiled chains.

DOI: 10.1021/acs.jpcb.9b06681
J. Phys. Chem. B 2019, 123, 10233–10244

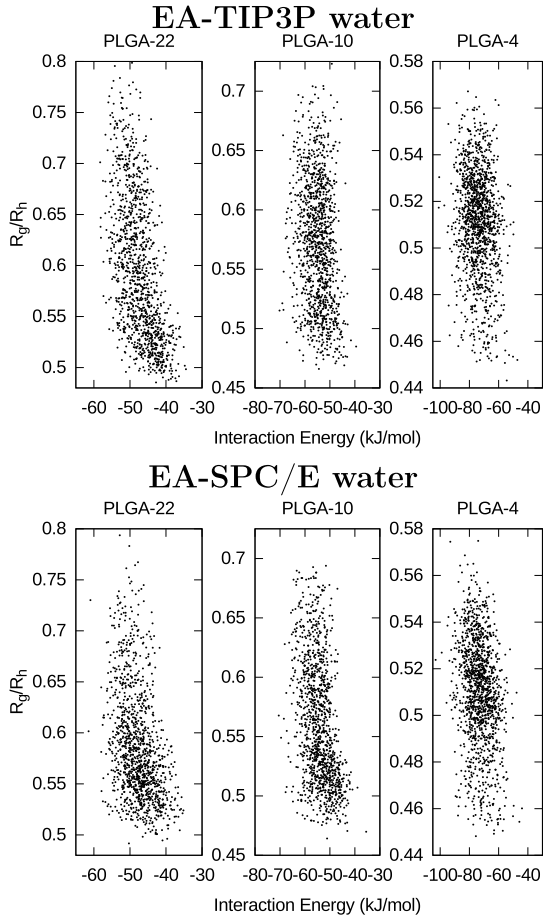

Figure 7. Ratio of the radius of gyration to the hydrodynamic radius of the PLGA oligomers in the mixed EA−water solution vs interaction energy per monomer along the 40 ns MD *NVE* runs of the seven different oligomers with RESP charges combined in one plot per size at 298 K. Top: EA-TIP3P, bottom: EA-SPC/E.

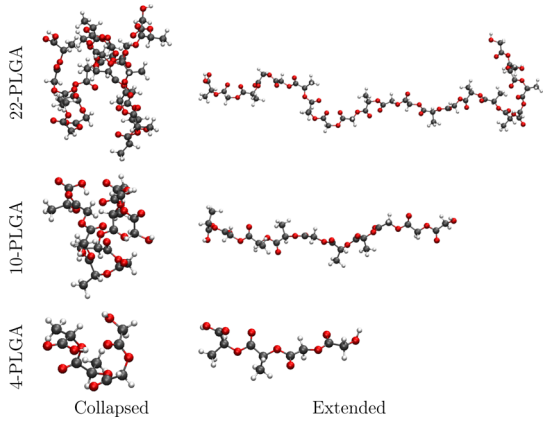

Figure 8. Renderings of instantaneous PLGA structures in the mixed EA−water solution. The R_r/R_{hyd} values of collapsed and extended structures are 0.48, 0.83 for 22-PLGA, 0.46, 0.73 for 10-PLGA, and 0.44, 0.58 for 4-PLGA.

7. DISCUSSION

It is quite evident that the fate of the structures of PLGA oligomers in the pure solvents is quite different, as described in detail in previous sections. It is also evident that these oligomers are more mobile in water than EA, although the values of the diffusion coefficient in TIP3P water might not be as realistic as in EA and SPC/E water. It is known that the self diffusion of TIP3P water does not compare well[45] with the experimental value of 2.299 cm^{-5}/s at 298 K.[29] The structural behavior in the mixed solvent 1:1.643 EA/water is interesting and points to important considerations if this mixture is used for the fabrication of PLGA particles. A further comparison between the three solvents can be obtained from the observation of the rdf between centers of mass of the PLGA oligomer and centers of mass of the water molecules. Figure 9 illustrates these rdf for the 22-PLGA oligomer in the three solvents studied here. Integrating these functions up to the minimum that follows the first maximum gives an approximate number of solvent molecules in the first coordination shell of each oligomer monomer. In the pure solvents, the coordination shell contains 7−8 EA molecules for the two types of charges (BCC or RESP) considered or 12−14 water molecules for the TIP3P and SPC/E water. However, in the mixed solvent, the coordination number ranges around 1−2 water molecules plus 7−8 EA molecules in the case of RESP charges and around 6−7 water molecules plus 3 EA molecules in the BCC case. Therefore, if the force field includes RESP charges, the 22-PLGA oligomer in the mixed system is accommodating in the first coordination shell roughly equal number of EA molecules than in the pure solvent with only a couple of water molecules. On the other hand, if the force field includes BCC charges, the mixed system accommodates in the first coordination shell roughly half of the number of molecules of each type than what it has in the pure solvents as shown in Figure 10.

For the BCC case, the top-left pane of Figure 10 shows a direct count of the mass of the EA (orange) and the water molecules (cyan) within a 6 Å distance from the 22-PLGA monomers in the mixed solvent along the last 39 ns of the *NVE* MD production simulation at 298 K. On average within that distance, the mass of EA molecules is 2.5×10^3 u and that of water molecules is 1.3×10^3 u, which yields a mixing ratio of 1.92:1.00 EA−water in molecular weight. This shows that in the immediate surroundings of the solute, there are about three times more EA molecules than expected if the 1:1.6 relative concentration of the two solvents would be uniform. For the RESP case, the mass mixing ratio is 18:1 EA−water showing that the immediate neighborhood of the solvated 22-PLGA is EA-rich. Altogether, the 22-PLGA oligomers prefer to remain within the liquid−liquid interface of the phase separated solvents with a tendency of being surrounded by EA molecules. As an example, Figure 10 illustrates the fluctuations over time of the total solvent mass within the oligomer neighborhood depicted in black or grey, with the black line corresponding to the solvent mass when the 22-PLGA oligomer is extended and grey line corresponding to collapsed oligomer structures. The presence of water molecules close to the oligomer is enough to favor its collapsed structure over longer periods of time than when the polymer is in pure EA. Figure 10 portrays the effect that different atomic charges (BCC or RESP) used in the modeling of the EA solvent has on the mixed solvent, showing that the RESP case favors more EA molecules in the immediate surroundings of the PLGA oligomers than the BCC case. Additionally, Figure 10 depicts two selected instantaneous structures of 22-PLGA and their local solvent surroundings, indicating that nonetheless the oligomer structure, the EA environment is dominant.

Summarizing, the most notable difference between BCC and RESP atomic charges in the GAFF is in the modeling of the pure EA. The RESP case is better, giving a clear liquid phase

DOI: 10.1021/acs.jpcb.9b06681
J. Phys. Chem. B 2019, 123, 10233−10244

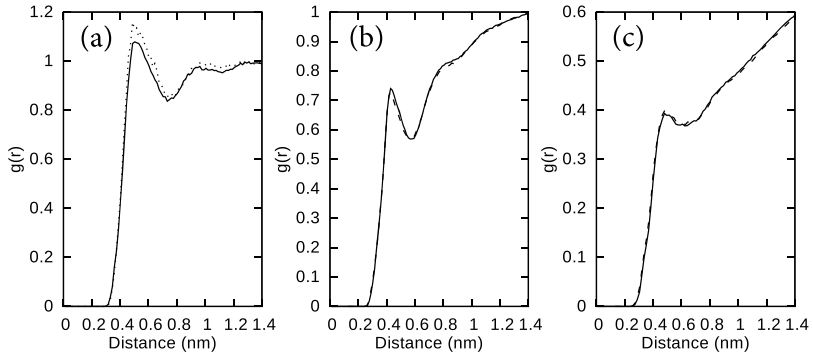

Figure 9. Pair distribution function of solvated 22-PLGA in three solvents. Functions are calculated between the center of mass of the oligomer monomers and the center of mass of the solvent molecules, at 298 K and the equilibrium density of each system. (a) Solvent is EA modeled with BCC atomic charges (solid line) and RESP atomic charges (dashed line); (b) solvent is water modeled with TIP3P (solid line) and SPC/E (dashed line); and (c) mixed EA−water solvent with TIP3P water (solid line) and SPC/E water (dashed line) and RESP atomic charges for EA.

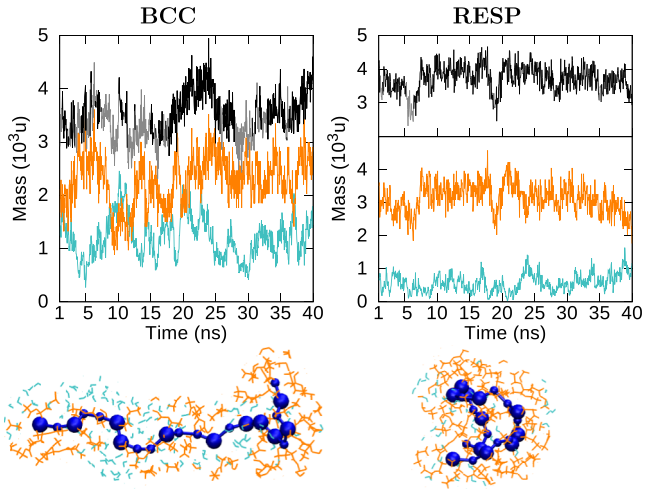

Figure 10. Top: EA and water molecules mass within a 6 Å shell surrounding 22-PLGA in mixed EA−water solvent at 298 K along the last 39 ns of *NVE* MD. Mixed solvent depicted has TIP3P water and EA modeled with BCC charges (left) or with RESP charges (right) with EA mass (orange), water mass (cyan), and total mass (black for extended oligomer, grey for collapsed oligomer). Bottom: Instantaneous solvent surroundings of 22-PLGA model A in extended (left) and collapsed (tight) structures, with large blue spheres corresponding to lactic acid monomers and small spheres corresponding to the glycolic monomers.

separation when mixed with either TIP3P or SPC/E water. Meanwhile, no major differences were detected between the effect on the structure of the PLGA oligomers solvated in either TIP3P or SPC/E water. The latter yields better estimates of the PLGA oligomer diffusivity.

8. CONCLUSIONS

PLGA nanostructures are complex and differ when synthesized by different experimental protocols, all of them involving solvents. A better understanding of the PLGA behavior in solvent environments is crucial. Herein, we have provided an analytic framework equipped with a collection of computational tools that included all-atom MD simulations, quantum chemistry, and statistical methods for revealing the effect of three different solvents on PLGA oligomers of various lengths. We have developed parameters for the GAFF of EA that permit accurate MD simulations; its availability will be useful for the community of polymer scientists interested in using this solvent. We have shown two characteristic structures of the PLGA oligomers that occur preferentially in diluted solutions of EA, water, and a mixture of the two liquids. It was unraveled that PLGA oligomers prefer extended structures when solvated in EA changing to collapsed structures extremely seldom along the MD simulation. Meanwhile, both oligomer structures are present when the oligomers are in water, favoring collapsed structures that are significantly slower to extend than in EA. Therefore, the oligomer changed shape less often in EA than in water. In the case of the mixed EA−water solvents, oligomers in the extended structure were trapped at the interface of the liquid−liquid phase separated solvents but could take on either extended or collapsed structures at different times with a high propensity of remaining in a local environment rich in EA molecules. Structural properties of the extended and collapsed structures such as the radius of gyration, hydrodynamic radius, end-to-end distance, orientational order parameter, flexibility coefficient, potential energy and polymer−solvent interaction energies are included in this work.

The insight obtained here will benefit applications involving the parent PLGA polymer of different lactic to glycolic ratios and lengths. We predict that in oligomers where several lactic acid monomers are contiguous the folded structures will be favored, similarly to previous predictions for pure lactic acid short oligomers.[7] The experimental process for obtaining asymmetric nanoparticles and dendrons[8,9] involves microstructures that form in the organic phase and precipitate as the solvent phase evaporates. Our findings are important in the design of such nanostructures as well as in the control of polymer folding when devising scaffoldings for tissue engineering and genetically engineered polymers.

APPENDIX 1

Table A1 gives average values of the structural and energetic properties of the various PLGA oligomers in the three studied solvents, EA, water, and a mixture of the two. Two sets of atomic charges are used in the GAFF for both, EA and PLGA oligomers, BCC and RESP. Two force fields are used for water, TIP3P, and SPC/E. The reported error of these properties corresponds to their standard deviation from values stored in 2000 saved configurations along the simulation. This is only a rough estimate because the distribution of property values can be fitted to two normal distributions associated to extended and collapsed structures.

DOI: 10.1021/acs.jpcb.9b06681
J. Phys. Chem. B 2019, 123, 10233−10244

Table A1. Average Properties and Standard Deviation of the Structural and Energy Properties for the Seven PLGA Oligomers Studied in This Work at 298 ± 2[a]

solvent	polymer	R_g (nm)	R_{hyd} (nm)	R_{ee} (nm)	Z	I_A (10^{-4} kg/m^2)	I_B/I_A	I_C/I_A	PE (kJ/mol)	E_{int} (kJ/mol)
	4-PLGA	0.42 ± 0.03	0.79 ± 0.02	1.0 ± 0.2	0.5 ± 0.2	1.3 ± 0.3	4.4 ± 0.9	4.9 ± 0.7	70 ± 5	−70 ± 5
EA	10-PLGA	0.7 ± 0.1	1.22 ± 0.06	1.8 ± 0.6	0.2 ± 0.2	12 ± 4	3.9 ± 1.4	4.5 ± 1.3	63 ± 3	−59 ± 4
(BCC)	22-PLGA	1.2 ± 0.2	1.8 ± 0.2	3.0 ± 1.0	0.1 ± 0.1	69 ± 23	3.9 ± 1.8	4.4 ± 1.8	62 ± 3	−53 ± 4
	4-PLGA	0.39 ± 0.02	0.78 ± 0.02	1.0 ± 0.2	0.4 ± 0.2	1.3 ± 0.3	4.2 ± 0.7	4.7 ± 0.7	124 ± 5	−69 ± 6
EA	10-PLGA	0.7 ± 0.1	1.20 ± 0.07	1.7 ± 0.6	0.1 ± 0.2	11 ± 4	3.7 ± 1.5	4.3 ± 1.5	78 ± 5	−52 ± 4
(RESP)	22-PLGA	1.08 ± 0.24	1.75 ± 0.16	2.55 ± 1.12	0.07 ± 0.11	64 ± 20	3.6 ± 2.0	4.1 ± 2.0	66 ± 6	−46 ± 3
	4-PLGA	0.39 ± 0.03	0.78 ± 0.02	0.9 ± 0.2	0.4 ± 0.2	1.4 ± 0.4	3.6 ± 1.0	4.1 ± 0.8	74 ± 6	−90 ± 10
TIP3P water	10-PLGA	0.6 ± 0.08	1.12 ± 0.07	1.2 ± 0.5	0.1 ± 0.2	11 ± 3	2.6 ± 1.1	3.1 ± 1.2	63 ± 4	−70 ± 6
(BCC)	22-PLGA	0.8 ± 0.1	1.46 ± 0.09	1.5 ± 0.6	0.0 ± 0.1	47 ± 10	2.1 ± 0.8	2.5 ± 0.9	60 ± 3	−58 ± 5
	4-PLGA	0.39 ± 0.03	0.78 ± 0.02	0.9 ± 0.2	0.3 ± 0.2	1.5 ± 0.4	3.3 ± 0.9	3.8 ± 0.8	74 ± 6	−92 ± 10
SPC/E water	10-PLGA	0.6 ± 0.07	1.11 ± 0.06	1.1 ± 0.5	0.04 ± 0.1	11 ± 2	2.5 ± 1.0	3.0 ± 1.0	63 ± 4	−74 ± 6
(BCC)	22-PLGA	0.7 ± 0.1	1.43 ± 0.08	1.4 ± 0.6	0.0 ± 0.1	45 ± 9	2.0 ± 0.8	2.3 ± 0.8	57 ± 3	−59 ± 5
	4-PLGA	0.39 ± 0.02	0.78 ± 0.02	0.8 ± 0.2	0.3 ± 0.2	1.6 ± 0.3	2.9 ± 0.8	3.4 ± 0.6	126 ± 6	−83 ± 8
TIP3P water	10-PLGA	0.56 ± 0.06	1.09 ± 0.05	1.1 ± 0.4	0.1 ± 0.1	10 ± 2	2.9 ± 0.8	2.4 ± 0.6	78 ± 5	−60 ± 5
(RESP)	22-PLGA	0.69 ± 0.06	1.39 ± 0.06	1.3 ± 0.5	0.03 ± 0.10	44.5 ± 6.4	1.7 ± 0.5	2.0 ± 0.5	62 ± 6	−46 ± 4
	4-PLGA	0.38 ± 0.03	0.77 ± 0.02	0.8 ± 0.2	0.2 ± 0.2	1.7 ± 0.3	2.4 ± 0.7	3.0 ± 0.6	125 ± 5	−85 ± 9
SPC/E water	10-PLGA	0.54 ± 0.04	1.07 ± 0.04	0.9 ± 0.3	0.0 ± 0.1	10.0 ± 1.9	2.4 ± 0.7	3.0 ± 0.7	78 ± 5	−63 ± 5
(RESP)	22-PLGA	0.68 ± 0.06	1.38 ± 0.05	1.1 ± 0.4	0.0 ± 0.1	43 ± 6	1.7 ± 0.5	2.0 ± 0.5	62 ± 6	−47 ± 4
	4-PLGA	0.4 ± 0.03	0.78 ± 0.02	0.9 ± 0.2	0.4 ± 0.2	1.4 ± 0.4	4.0 ± 1.0	4.5 ± 0.8	73 ± 6	−90 ± 10
EA-water	10-PLGA	0.7 ± 0.1	1.19 ± 0.07	1.6 ± 0.6	0.1 ± 0.3	11 ± 3	3.6 ± 1.5	4.1 ± 1.4	63 ± 3	−59 ± 4
(BCC, TIP3P)	22-PLGA	0.9 ± 0.2	1.6 ± 0.1	2.0 ± 0.8	0.1 ± 0.1	57 ± 17	2.9 ± 1.4	3.3 ± 1.4	62 ± 3	−53 ± 4
	4-PLGA	0.40 ± 0.02	0.78 ± 0.02	1.0 ± 1.8	0.5 ± 0.2	1.3 ± 0.3	4.4 ± 0.9	4.9 ± 0.8	74 ± 6	−88 ± 10
EA-water	10-PLGA	0.65 ± 0.09	1.17 ± 0.07	1.5 ± 0.6	0.09 ± 0.2	12 ± 3	3.1 ± 1.2	3.6 ± 1.2	63 ± 4	−70 ± 6
(BCC, SPC/E)	22-PLGA	1.0 ± 0.2	1.7 ± 0.2	2.4 ± 1.2	0.1 ± 0.1	56 ± 16	4.0 ± 2.5	4.5 ± 2.5	62 ± 3	−61 ± 4
	4-PLGA	0.41 ± 0.02	0.79 ± 0.01	1.0 ± 0.2	0.4 ± 0.2	1.4 ± 0.3	3.7 ± 0.8	4.2 ± 0.7	123 ± 5	−74 ± 8
EA-water	10-PLGA	0.68 ± 0.10	1.19 ± 0.07	1.7 ± 0.6	0.1 ± 0.2	11.2 ± 3.4	3.6 ± 1.5	4.1 ± 1.4	80 ± 4	−59 ± 5
(RESP, TIP3P)	22-PLGA	1.01 ± 0.20	1.7 ± 0.1	2.5 ± 1.0	0.1 ± 0.1	61 ± 20	3.7 ± 1.8	4.2 ± 1.8	67 ± 6	−49 ± 3
	4-PLGA	0.40 ± 0.02	0.79 ± 0.02	1.0 ± 0.2	0.4 ± 0.2	1.4 ± 0.3	3.3 ± 1.4	4.3 ± 0.7	124 ± 5	−79 ± 8
EA-water	10-PLGA	0.68 ± 0.10	1.19 ± 0.07	1.6 ± 0.6	0.1 ± 0.2	11.7 ± 3.7	3.3 ± 1.7	3.9 ± 1.4	77 ± 7	−54 ± 4
(RESP, SPC/E)	22-PLGA	1.0 ± 0.2	1.7 ± 0.1	2.3 ± 1.0	0.1 ± 0.1	63 ± 20	3.0 ± 1.5	3.7 ± 1.6	67 ± 6	−48 ± 4

[a]PE and E_{int} are values per monomer.

■ ASSOCIATED CONTENT

Supporting Information

The Supporting Information is available free of charge at https://pubs.acs.org/doi/10.1021/acs.jpcb.9b06681.

Details on the PLGA oligomers structure used to obtain the RESP atomic charges; plots of the distribution of charge within each oligomer and multiple plots showing the time evolution of each PLGA oligomer during the *NVE*-MD production runs in EA; TIP3P water, SPC/E water, and the mixture EA−water; EA topology file for the GAFF parameters with the calculated RESP charges for the EA liquid; and seven topology files for the GAFF with the calculated RESP charges for 22-PLGA, models A, B, C, for the 10-PLGA, models I, J, K, and for 4-PLGA (PDF)

■ AUTHOR INFORMATION

Corresponding Author

*E-mail: blaisten@gmu.edu.

ORCID

Estela Blaisten-Barojas: 0000-0003-3259-1573

Notes

The authors declare no competing financial interest.

■ ACKNOWLEDGMENTS

We acknowledge partial support from the Thomas F. and Kate Miller Jeffress Memorial Trust. J.A. gratefully acknowledges his doctoral scholarship support from the Provost Office. Some initial calculations for the 4-PLGA oligomer by Muhammad Namasi are acknowledged. All computations were done in the Argo cluster of the Office of Research Computing at George Mason University.

DOI: 10.1021/acs.jpcb.9b06681
J. Phys. Chem. B 2019, 123, 10233−10244

REFERENCES

(1) Fathi, M.; Barar, J. Perspective Highlights on Biodegradable Polymeric Nanosystems for Targeted Therapy of Solid Tumors. *BioImpacts* **2017**, *7*, 49−57.

(2) Kumari, A.; Yadav, S. K.; Yadav, S. C. Biodegradable polymeric nanoparticles based drug delivery systems. *Colloids Surf., B* **2010**, *75*, 1−18.

(3) Astete, C. E.; Sabliov, C. M. Synthesis and characterization of PLGA nanoparticles. *J. Biomater. Sci., Polym. Ed.* **2006**, *17*, 247−289.

(4) Bala, I.; Hariharan, S.; Kumar, M. N. V. R. PLGA Nanoparticles in Drug Delivery: The State of the Art. *Crit. Rev. Ther. Drug Carrier Syst.* **2004**, *21*, 387−422.

(5) Wang, N.; Wu, X. S. Lactic-Glycolic Acid Oligomeric Microgranules for Aspirin Delivery and Stabilization. In *Tailored Polymeric Materials for Controlled Delivery Systems*; McCulloch, W., Shalaby, S. I., Eds.; American Chemical Society: Washington DC, 1998; Vol. *709*, pp 254−264.

(6) Takizawa, K.; Nulwala, H.; Hu, J.; Yoshinaga, K.; Hawker, C. J. Molecularly Defined (L)-Lactic Acid Oligomers and Polymers: Synthesis and Characterization. *J. Polym. Sci., Part A: Polym. Chem.* **2008**, *46*, 5977−5990.

(7) Hongen, T.; Taniguchi, T.; Nomura, S.; Kadokawa, J.-i.; Monde, K. In Depth Study on Solution-State Structure of Poly(lactic acid) by Vibrational Circular Dichroism. *Macromolecules* **2014**, *47*, 5313−5319.

(8) Santos, J. L.; Herrera-Alonso, M. Kinetically Arrested Assemblies of Architecturally Distinct Block Copolymers. *Macromolecules* **2014**, *47*, 137−145.

(9) Salvador-Morales, C.; Brahmbhatt, B.; Márquez-Miranda, V.; Araya-Duran, I.; Canan, J.; Gonzalez-Nilo, F.; Vilos, C.; Cebral, J.; Mut, F.; Lohner, R.; et al. Mechanistic Studies on the Self-Assembly of PLGA Patchy Particles and Their Potential Applications in Biomedical Imaging. *Langmuir* **2016**, *32*, 7929−7942.

(10) Pei, K.; Ying, Y.; Chu, C. Molecular dynamic simulations of a new family of synthetic biodegradable amino acid-based poly(ester amide) biomaterials: Glass transition temperature and adhesion behavior. *Mater. Today Chem.* **2017**, *4*, 90−96.

(11) Metwally, A. A.; Hathout, R. M. Computer-Assisted Drug Formulation Design: Novel Approach in Drug Delivery. *Mol. Pharm.* **2015**, *12*, 2800−2810.

(12) Gentile, P.; Chiono, V.; Carmagnola, I.; Hatton, P. An Overview of Poly(lactic-co-glycolic) Acid (PLGA)-Based Biomaterials for Bone Tissue Engineering. *Int. J. Mol. Sci.* **2014**, *15*, 3640−3659.

(13) Lanao, R. P. F.; Jonker, A. M.; Wolke, J. G. C.; Jansen, J. A.; van Hest, J. C. M.; Leeuwenburgh, S. C. G. Physicochemical Properties and Applications of Poly(lactic-co-glycolic acid) for Use in Bone Regeneration. *Tissue Eng., Part B* **2013**, *19*, 380−390.

(14) Gilding, D. K.; Reed, A. M. Biodegradable polymers for use in surgery-polyglycolic/poly(actic acid) homo- and copolymers: 1. *Polymer* **1979**, *20*, 1459−1464.

(15) Makadia, H. K.; Siegel, S. J. Poly Lactic-co-glycolic Acid (PLGA) as Biodegradable Controlled Drug Delivery Carrier. *Polymers* **2011**, *3*, 1377−1397.

(16) Case, D. A.; Betz, R. M.; Cerutti, D. S.; Cheatham, T. E., III; Darden, T. A.; Duke, R. E.; Giese, T. J.; Gohlke, H.; Goetz, A. W.; Homeyer, N.; et al. *AMBER 16*; University of California: San Francisco, CA, 2016.

(17) Jakalian, A.; Bush, B. L.; Jack, D. B.; Bayly, C. I. Fast, Efficient Generation of High-Quality Atomic Charges. AM1-BCC model: I. Method. *J. Comput. Chem.* **2000**, *21*, 132−146.

(18) Jakalian, A.; Jack, D. B.; Bayly, C. I. Fast, Efficient Generation of High-Quality Atomic Charges. AM1-BCC Model: II. Parameterization and Validation. *J. Comput. Chem.* **2002**, *23*, 1623−1641.

(19) Singh, U. C.; Kollman, P. A. An Approach to Computing Electrostatic Charges for Molecules. *J. Comput. Chem.* **1984**, *5*, 129−145.

(20) Besler, B. H.; Merz, K. M., Jr.; Kollman, P. A. Atomic Charges Derived from Semiempirical Methods. *J. Comput. Chem.* **1990**, *11*, 431−439.

(21) Frisch, M. J.; Trucks, G. W.; Schlegel, H. B.; Scuseria, G. E.; Robb, M. A.; Cheeseman, J. R.; Scalmani, G.; Barone, V.; Mennucci, B.; Petersson, G. A.; et al. *Gaussian 09*, Revision A.1; Gaussian, Inc.: Wallingford, CT, 2009.

(22) Jorgensen, W. L.; Chandrasekhar, J.; Madura, J. D.; Impey, R. W.; Klein, M. L. Comparison of Simple Potential Functions for Simulating Liquid Water. *J. Chem. Phys.* **1983**, *79*, 926−935.

(23) Berendsen, H. J. C.; Grigera, J. R.; Straatsma, T. P. The Missing Term in Effective Pair Potentials. *J. Phys. Chem.* **1987**, *91*, 6269−6271.

(24) *GROMACS 2018*. http://www.gromacs.org, 2018 (accessed Sep 30, 2019).

(25) Usatenko, Z.; Sommer, J.-U. Calculation of the Segmental Order Parameter for a Polymer Chain in Good Solvent. *Macromol. Theory Simul.* **2008**, *17*, 39−44.

(26) Dai, Y.; Blaisten-Barojas, E. Monte Carlo Study of Oligopyrroles in Condensed Phases. *J. Chem. Phys.* **2010**, *133*, 034905.

(27) Tanford, C. *Physical Chemistry of Macromolecules*; John Wiley & Sons Inc.: New York, NY, USA, 1961.

(28) Yeh, I.-C.; Hummer, G. System-Size Dependence of Diffusion Coefficients and Viscosities from Molecular Dynamics Simulations with Periodic Boundary Conditions. *J. Phys. Chem. B* **2004**, *108*, 15873−15879.

(29) *CRC Handbook of Chemistry and Physics*, 99th ed.; Rumble, J. R., Ed.; CRC Press LLC: Boca Raton, Forida, 2019.

(30) Zábranský, M.; Hynek, V.; Finkeová-Haštabová, J.; Veselý, F. Heat Capacities of Six Liquid Esters as a Function of Temperature. *Collect. Czech. Chem. Commun.* **1987**, *52*, 251−257.

(31) Uminski, T.; Dera, J.; Kupryszewski, G. The Measurement of Self-Diffusion Coefficient in Dielectric Liquids Using the Method of Open-Ended Capillaries and Radioisotope Technique. *Acta Phys. Pol.* **1965**, *28*, 17−24.

(32) Wilke, C. R.; Chang, P. Correlation of Diffusion Coefficients in Dilute Solutions. *AIChE J.* **1955**, *1*, 264−270.

(33) van der Bruggen, B.; Schaep, J.; Wilms, D.; Vandecasteele, C. Influence of Molecular Size, Polarity and Charge on the Retention of Organic Molecules by Nanofiltration. *J. Membr. Sci.* **1999**, *156*, 29−41.

(34) Wilson, M. R. Determination of Order Parameters in Realistic Atom-Based Models of Liquid Crystal Systems. *J. Mol. Liq.* **1996**, *68*, 23−31.

(35) Caleman, C.; van Maaren, P. J.; Hong, M.; Hub, J. S.; Costa, L. T.; van der Spoel, D. Force Field Benchmark of Organic Liquids: Density, Enthalpy of Vaporization, Heat Capacities, Surface Tension, Isothermal Compressibility, Volumetric Expansion Coefficient, and Dielectric Constant. *J. Chem. Theory Comput.* **2012**, *8*, 61−74.

(36) Flory, P. J. *Principles of Polymer Chemistry*; Cornell University Press: Ithaca, New York, 1953.

(37) Rollings, J. E. Use of on-line Laser Light Scattering Coupled to Chromatographic Separations for the Determination of Molecular Weight, Branching, Size, and Shape Distribution in Polysaccharides. In *Laser Light Scattering in Biochemistry*; Harding, S. E., Sattelle, D. B., Bloomfield, V. A., Eds.; The Royal Society of Chemistry: Cambridge, U. K., 1992; pp 275−293.

(38) Casalini, T.; Rossi, F.; Santoro, M.; Perale, G. Structural Characterization of Poly-L-lactic Acid (PLLA) and Poly(glycolic acid)(PGA) Oligomers. *Int. J. Mol. Sci.* **2011**, *12*, 3857−3870.

(39) Burchard, W.; Schmidt, M.; Stockmayer, W. H. Information on Polydispersity and Branching from Combined Quasi-Elastic and Intergrated Scattering. *Macromolecules* **1980**, *13*, 1265−1272.

(40) Wilkins, D. K.; Grimshaw, S. B.; Receveur, V.; Dobson, C. M.; Jones, J. A.; Smith, L. J. Hydrodynamic Radii of Native and Denatured Proteins Measured by Pulse Field Gradient NMR Techniques. *Biochemistry* **1999**, *38*, 16424−16431.

(41) Vega, C.; Abascal, J. L. F. Relation Between the Melting Temperature and the Temperature of Maximum Density for the Most Common Models of Water. *J. Chem. Phys.* **2005**, *123*, 144504.

(42) Price, D. J.; Brooks, C. L., III A modified TIP3P water potential for simulation with Ewald summation. *J. Chem. Phys.* **2004**, *121*, 10096.

(43) Ribeiro, A. C. F.; Lobo, V. M. M.; Leaist, D. G.; Natividade, J. J. S.; Veríssimo, L. P.; Barros, M. C. F.; Cabral, A. M. T. D. P. V. Binary

DOI: 10.1021/acs.jpcb.9b06681
J. Phys. Chem. B 2019, 123, 10233−10244

Diffusion Coefficients for Aqueous Solutions of Lactic Acid. *J. Solution Chem.* **2005**, *34*, 1009−1016.
(44) Wasik, S. P.; Tewari, Y. B.; Miller, M. M.; Martire, D. E. *Octanol/Water Partition Coefficients and Aqueous Solubilities of Organic Compounds*. Report of the U.S. Department of Commerce, NBSIR 81-2406, 1981; p 66.
(45) Mark, P.; Nilsson, L. Structure and Dynamics of the TIP3P, SPC, and SPC/E Water Models at 298 K. *J. Phys. Chem. A* **2001**, *105*, 9954−9960.

DOI: 10.1021/acs.jpcb.9b06681
J. Phys. Chem. B 2019, 123, 10233−10244